

New approach to study light-emission of periodic structures. Unveiling novel surface-states effects

Pedro Pereyra

Física Teórica y Materia Condensada, UAM-Azcapotzalco, C.P. 02200, México D. F., México

(Dated: September 3, 2018)

An accurate approach to calculate the optical response of periodic structures is proposed. Using the genuine superlattice eigenfunctions and energy eigenvalues, the eigenfunctions parity symmetries, the subband symmetries and the detached surface energy levels, we report new optical-transition selection rules and explicit optical-response calculations. Observed transitions that were considered forbidden, become allowed and interesting optical-spectra effects emerge as fingerprints of intra-subband and surface states. The unexplained groups and isolated narrow peaks observed in high resolution blue-laser spectra, by Nakamura et al., are now fully explained and faithfully reproduced.

PACS numbers: 03.65.Ge, 42.50.-p, 42.50.Ct, 42.62.Fi, 68.65.Ac, 73.20.-r, 78.30.Fs, 78.55.-m, 78.66.Fd, 78.67.Pt, 85.60.-q

Although the fascinating phenomenon of light emission has been studied for more than a century, the main problem in calculating optical responses of semiconductor periodic structures using, for example, the golden rule

$$|\langle \psi_f | H_{\text{int}} | \psi_i \rangle|^2 / [E_f - E_i + \hbar\omega]^2 + \Gamma_i^2 \quad (1)$$

where H_{int} describes the light-matter interaction and ω the emitted photon frequency, has been the lack of explicit knowledge of the initial and final states $|\psi_i\rangle$ and $|\psi_f\rangle$ and of the corresponding energies E_i and E_f .^{1,2} In the standard approaches (SAs) to periodic systems, based on models and theorems for infinite periodic systems,^{3–13} the energy levels become continuous bands or subbands (SBs). This return to a quasi-continuous-energy description is responsible, for example, for the theoretical inability to explain high resolution photoluminescence-spectra features, like those observed by Nakamura et al.²¹ and for approximate selection rules^{5,8,14} that lead to affirm that some observed transitions are “forbidden ones”.^{15–20}

We show here that using the eigenvalues $E_{\mu\nu}$ and eigenfunctions $\Psi_{\mu\nu}(z)$, rigorously obtained in the theory of finite periodic systems,²² and the eigenfunctions’ parity symmetries recently derived,²³ we not only replace the continuous subbands description of the standard approach by the most accurate discrete subbands description, we also unveil the surface energy levels (see figure 1), responsible for the, so far, unexplained optical-spectra effects observed in high resolution experiments. At the same time we recover a truly quantum description of optical emissions in periodic structures.

We will show that the detachment of the surface energy levels, apparent in figure 1, is responsible for the groups of peaks observed by Nakamura et al. We will present new selection rules, based on the eigenfunctions’ symmetries and strongly dependent on the quantum numbers μ and ν , the parity of n and on the surface states. The “forbidden transitions” will become allowed. We will report here two types of selection rules. The first one, based on the eigenfunction’s parity symmetry, will reduce the number of evaluations from $N \simeq (n+1)^2 n_c n_v$ to $N/2$, for a SL with n unit cells, n_c SBs in the conduction band (CB)

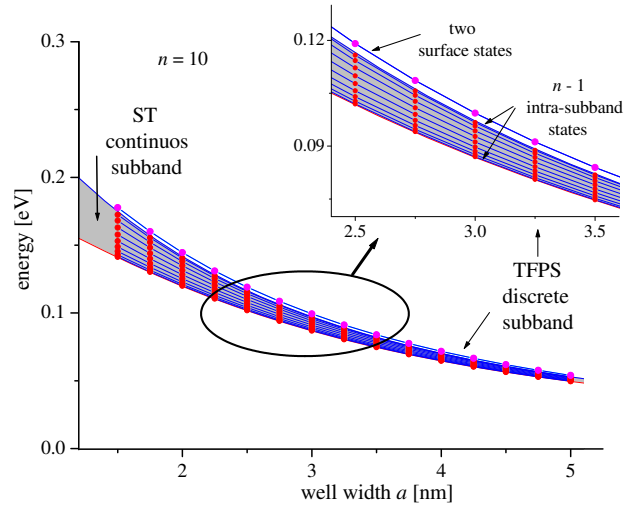


FIG. 1. Continuous and discrete first subband of the conduction band, as functions of the well width a , obtained for a Koronig-Penney-like periodic potential in the standard approach and in the TFPS, respectively. $n-1$ of the $n+1$ eigenvalues are true intra-subband energy levels and the remaining two are the energy levels of the surface states.

and n_v SBs in the valence band (VB). The second rule, based on the subband symmetry. This rule will reduce the number of evaluations to $\simeq nn_c n_v / 2$.

For simplicity we will refer here to type I SLs. The generalization is direct. It was shown in Ref.[22] that the eigenvalues, for SL bounded by cladding layers like in figure 2, can be obtained from

$$\Re(\alpha_n e^{ika}) - \frac{k^2 - q_w^2}{2q_w k} \Im(\alpha_n e^{ika}) - \frac{k^2 + q_w^2}{2q_w k} \Im\beta_n = 0, \quad (2)$$

where q_w and k are the wave numbers at the left (right) and right (left) of the discontinuity point z_L (z_R), $\alpha_n = U_n - \alpha^* U_{n-1}$ and $\beta_n = \beta U_{n-1}$ the n -cell transfer matrix elements, and U_n the Chebychev polynomial of the second kind evaluated at the real part of the matrix element

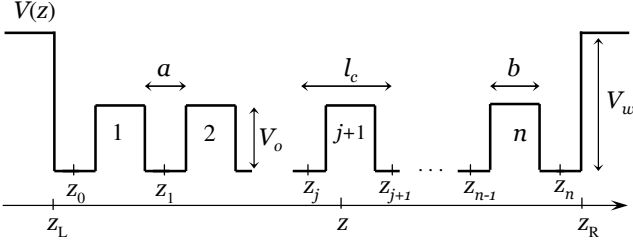


FIG. 2. Potential profile in the CB edge and parameters of a type I quasi-bounded superlattice. The wave function in Eq. (5) applies to a point z of the $j+1$ cell, with $0 \leq j \leq (n-1)$.

$M_{1,1}$ of the unit-cell transfer matrix

$$M(z_{i+1}, z_i) = \begin{pmatrix} \alpha & \beta \\ \beta^* & \alpha^* \end{pmatrix}. \quad (3)$$

The eigenfunctions, are obtained from

$$\Psi_{\mu,\nu}^{qb}(z) = \Psi^{qb}(z, E_{\mu,\nu}), \quad (4)$$

where

$$\Psi^{qb}(z, E) = \frac{a_o}{2k} \left[\left((\alpha_p + \gamma_p)\alpha_j + (\beta_p + \delta_p)\beta_j^* \right) e^{ika/2}(k - iq_w) + \left((\alpha_p + \gamma_p)\beta_j + (\beta_p + \delta_p)\alpha_j^* \right) e^{-ika/2}(k + iq_w) \right]. \quad (5)$$

Here a_o is a normalization constant and z any point in the $j+1$ cell, i.e. any point between z_j and z_{j+1} , with $0 \leq j \leq (n-1)$. α_j, β_j, \dots are the j -cells transfer-matrix elements and α_p, β_p, \dots the matrix elements of $M_p(z, z_j)$ that connects the state vectors $\Phi(z_j)$ and $\Phi(z)$, for $z_j \leq z \leq z_{j+1}$. The super-index q refers to quasi-bound superlattice and $b = c, v$ refers to conduction and valence band. The super-index q and the band index will be written only if they are necessary.

To evaluate the SL optical response, specifically the photoluminescence (PL) for specific systems, we will consider the golden rule

$$\chi_{PL}^r = \sum_{\nu, \nu', \mu, \mu'} f_{eh} \frac{\left| \int dz [\Psi_{\mu', \nu'}^{\nu}(z)]^* \frac{\partial}{\partial z} \Psi_{\mu, \nu}^c(z) \right|^2}{(\hbar\omega - E_{\mu, \nu}^c - E_g + E_{\mu', \nu'}^v + E_B)^2 + \Gamma^2}, \quad (6)$$

with energies measured from the corresponding band edges. Here E_g is the gap energy, E_B the exciton binding energy, Γ the level broadening energy and f_{eh} the occupation probability.

The parity symmetries, for eigenfunctions of quasi-bounded SLs, are summarized as²³

$$\Psi_{\mu, \nu}(z) = \begin{cases} (-1)^{\nu+1} \Psi_{\mu, \nu}(-z) & \text{for } n \text{ odd} \\ (-1)^{\nu+\mu} \Psi_{\mu, \nu}(-z) & \text{for } n \text{ even} \end{cases}. \quad (7)$$

These relations lead to the following symmetry selection rules (SSRs). For n even, we have:

$$\int dz \Psi_{\mu', \nu'}^v(z) \frac{\partial}{\partial z} \Psi_{\mu, \nu}^c(z) \begin{cases} = 0 & \text{when } P[\mu' + \nu'] = P[\mu + \nu]; \\ \neq 0 & \text{when } P[\mu' + \nu'] = P[\mu + \nu + 1]. \end{cases} \quad (8)$$

Here $P[l]$ means parity of l . When n is odd the SSRs are:

$$\int dz \Psi_{\mu', \nu'}^v(z) \frac{\partial}{\partial z} \Psi_{\mu, \nu}^c(z) \begin{cases} = 0 & \text{when } P[\nu'] = P[\nu]; \\ \neq 0 & \text{when } P[\nu'] = P[\nu + 1]. \end{cases} \quad (9)$$

Similar relations hold for IR transitions, with the additional restrictions $\mu \geq \mu'$ and, whenever $\mu = \mu'$, we must also have $\nu > \nu'$, see Ref. [24]. These rules, as mentioned before, effectively reduce the number of possible transitions to $N/2$. Depending on the number of subbands, this can be still a large number. To reduce even more the number of matrix-elements evaluations, we will introduce, some lines below, other rules related with the subband symmetry.

To test our approach, we will consider two specific examples, with results obtained with highest experimental resolution that we could find in the literature. In Ref. [21] the blue emitting SLs $(In_xGa_{1-x}N \setminus In_yGa_{1-y}N)^n \setminus In_xGa_{1-x}N$, bounded by GaN and $AlGaN$ cladding layers, with $x=0.2$, $y=0.05$ and different values of n , have been extensively studied. Some results, show spectral features, with groups of nar-

row spectral widths and peak separations of the order of 0.2nm (~ 0.12 meV), that could not be explained so far.

In the upper panel of figure 3, the PL spectrum, first published in Ref. [25], for a SL with $n=10$ and using a monochromator resolution²⁵ of 0.016nm (~ 0.01 meV) is shown. Taking into account this SL parameters, and the appropriate electron and hole effective masses, we obtain the energy eigenvalues, the eigenfunctions and the PL spectrum plotted in the middle panel of figure 3. Some eigenfunctions $\Psi_{1, \nu}^c$, in the first SB of the CB, are plotted in figure 4. Notice that the eigenvalues $E_{1,10}^c$ and $E_{1,11}^c$, that correspond to the surface states $\Psi_{1,10}^c$ and $\Psi_{1,11}^c$, are detached from the others energy levels in the SB.

To understand the structure of the optical response in figure 3 let us distinguish, in each subband μ of the CB, the surface energy levels $\{s\mu\}$ from the remaining $n-1$ energy levels $\{g\mu\}$. Similarly, the energy levels $\{s\mu'\}$ from

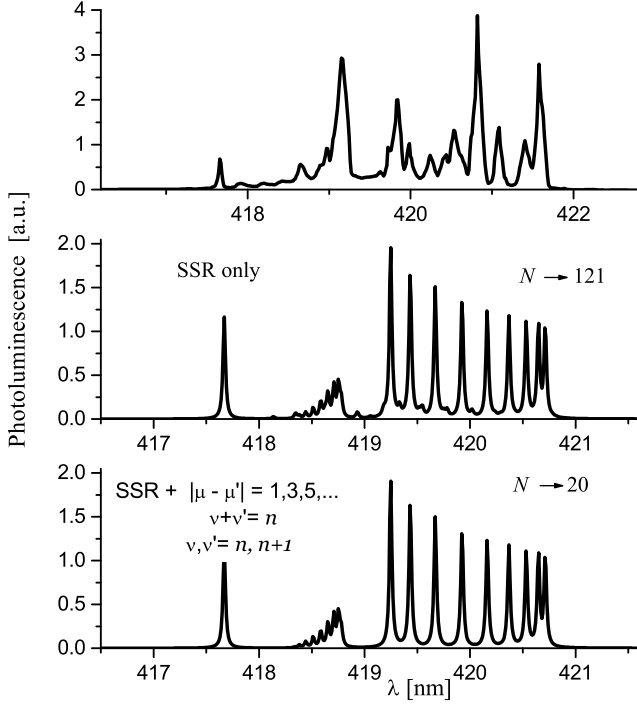


FIG. 3. Predicted and experimental PL spectra. Narrow and grouped peaks in the high resolution spectra measured by Nakamura et al.^{21,25} (upper panel) for the blue emitting $GaN \setminus (In_{0.2}Ga_{0.8}N \setminus In_{0.05}Ga_{0.95}N)^n \setminus GaN$ superlattice with $n=10$, $a=2.5\text{nm}$ and $b=5\text{nm}$, and our theoretical calculation (middle and lower panels). The experimental spectrum is reproduced with permission from [25]. Copyright [1996], AIP Publishing LLC.

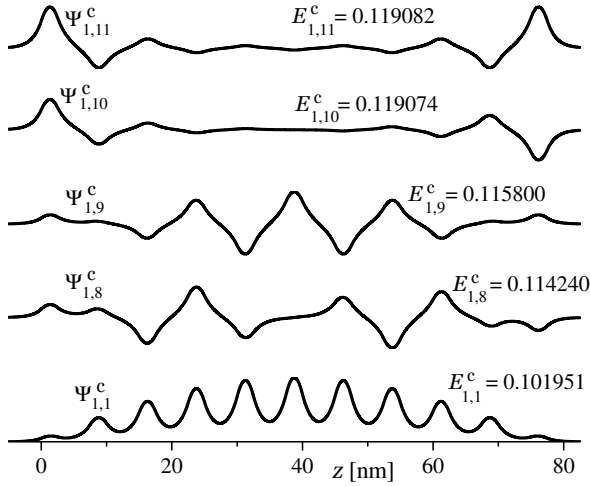


FIG. 4. Eigenfunctions and surface states. The eigenfunctions $\Psi_{1,1}^c(z)$, $\Psi_{1,8}^c(z)$ and $\Psi_{1,9}^c(z)$, and the slightly detached surface states $\Psi_{1,10}^c(z)$, and $\Psi_{1,11}^c(z)$ in the first subband of the CB of the blue emitting $(In_{0.2}Ga_{0.8}N \setminus In_{0.05}Ga_{0.95}N)^{10} \setminus In_{0.2}Ga_{0.8}N$ SL with $a=2.5\text{nm}$ and $b=5\text{nm}$, bounded by GaN cladding layers.

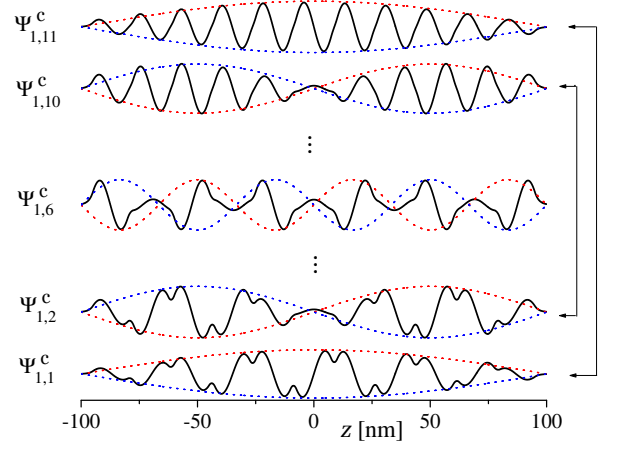


FIG. 5. The subband symmetry. Because of this symmetry the envelopes of the eigenfunctions with indices (μ, ν) and $(\mu, n+2-\nu)$ are the same. See for example $\Psi_{2,2}$ and $\Psi_{2,10}$. Here we plot the eigenfunctions $\Psi_{2,\nu}$ for a SL with $n=10$, thus with $\nu=1, 2, \dots, 11$.

the levels $\{g\mu'\}$, in the subband μ' of the VB. The transitions $g1 \rightarrow g2'$ are responsible for the group of peaks with larger wavelengths, between 419.24nm and 420.747nm, the transitions $g1 \rightarrow s2'$ and $s1 \rightarrow g2'$, for the group of peaks in the middle, and the transitions $s1 \rightarrow s2'$ for the isolated peak at the left.

This non-obvious resonant structure is a consequence of the presence of surface states, whose detachment determines the shift and the appearance of groups of peaks, as well as, of the isolated peak at a higher energy. It is clear that in order to observe this effect we need high-resolution experiments.

A rather general characteristic of the PL and IR spectra, measured or calculated, is the small number of peaks, much smaller than the $N/2$. One reason is, of course, the low experimental resolution. From the explicit calculations, we found out that, besides the parity symmetry, we have also the subband symmetry, glimpsed in Ref. [22], playing an important role in the relative values of the transition-matrix elements. In fact, when the surface levels detach, the matrix elements that fulfill the conditions

$$\begin{aligned} |\mu - \mu'| &= 1, 3, 5, \dots \\ &\text{and} \\ \langle \mu', \nu' | \frac{\partial}{\partial z} | \mu, \nu \rangle &\text{ with } \begin{aligned} \nu + \nu' &= n \\ \nu = n, n+1 &\quad \nu' = 1, 2, \dots \\ \nu = n, n+1 &\quad \nu = 1, 2, \dots, \end{aligned} \end{aligned} \quad (10)$$

are leading order transitions. When the surface levels do not detach, the leading order transitions are

$$\langle \mu', \nu' | \frac{\partial}{\partial z} | \mu, \nu \rangle \text{ where } \begin{aligned} |\mu - \mu'| &= 1, 3, 5, \dots \\ &\text{with} \\ \nu + \nu' &= n, n+2. \end{aligned} \quad (11)$$

Because of the subband symmetry, the envelope curve of $\Psi_{\mu,\nu}$ is similar to that of $\Psi_{\mu, n+2-\nu}$, when the SSs do not

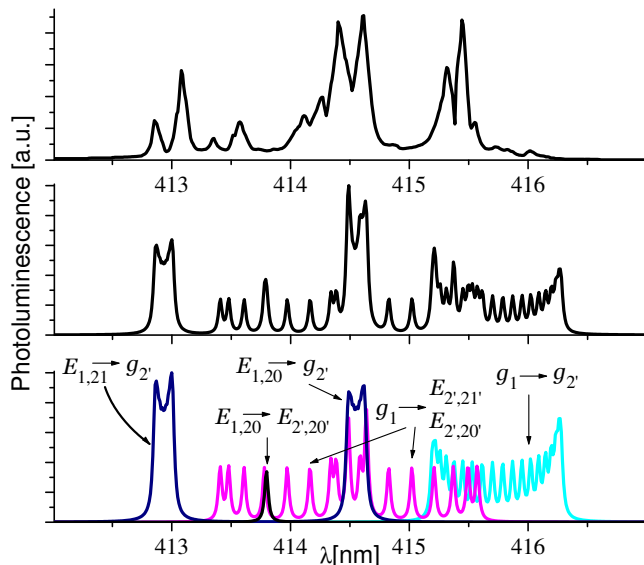


FIG. 6. Experimental²⁶ and theoretical PL spectra, upper and middle panels respectively, for a *GaInN* SL similar to the one considered for figure 3, but here with $n = 20$ and asymmetric confining potential, thus larger SSs detachment. In the lower panel we plot separately, and indicate, the transitions that contribute to the PL in the middle panel. It is clear that without the detachment of the surface energy levels, $E_{1,21}$, $E_{1,20}$, $E_{2',20'}$ and $E_{2',21'}$, we would not account the experimental behavior and we will have a spectrum similar to that of the transitions $g_1 \rightarrow g_2'$, only. The experimental curve with permission of The Japan Society of Applied Physics, Copyright 1996.

detach, and similar to that of $\Psi_{\mu,n-\nu}$, when they detach. The eigenfunctions in figure 5, correspond to a system where the SSs do not detach. In the blue emitting SL studied here the SSs detach, see figure 4.

The leading order rules (LORs) reduce the number of matrix-elements evaluations. For a PL spectrum, the reduction is from $N/2 \simeq (n+1)^2 n_c n_v / 2$ to $\simeq n n_c n_v$, in the first case, and to $(n+1) n_c n_v$, in the second. To obtain the IR spectra we have, additionally, the condition $\mu' \leq \mu$.

If we apply the LORs for our example, with $n = 10$,

$n_c=1$ and $n_v=2$, the number of matrix-elements evaluations reduces from $(n+1)^2 n_v / 2 = 121$ to $n n_c n_v = 20$. The new spectrum, shown in the lower panel of figure 3, contains essentially the same information as the one in the center. At the end, the number of transition matrix-elements that we calculate, using the SSRs and the LORs, is the same as the number of peaks in the actual PL spectra.

In figure 6 we have the experimental and theoretical PL spectra for another sample in Yakamura's et al. book, first published in Ref. [26]. In this case the number of unit cells, $n=20$, implies 882 matrix-elements evaluations. In the upper panel we show the spectrum (c) of figure 11.10 in Reference [21]. To account for this result we had to take into account the confining potential asymmetry. Because of this asymmetry, the surface energy levels split and the surface states lose their parity symmetry. The other eigenvalues and eigenfunctions remain almost unchanged. Thus, the SSRs are still valid for the $g_1 \rightarrow g_2'$ transitions, but not for the $E_{1,21} \rightarrow g_2'$ and $E_{1,20} \rightarrow g_2'$ transitions. The surface states $\Psi_{1,20}$ and $\Psi_{1,21}$ in $s1$ become localized at the opposite sides of the superlattice. The same happens with $\Psi_{2',20'}$ and $\Psi_{2',21'}$. Even so, using the SSRs and the LORs we end up calculating 78 matrix-elements and with the spectrum in the panel at the middle of figure 6. As shown in the lower panel of this figure, the transitions $E_{1,21} \rightarrow g_2'$ and $E_{1,20} \rightarrow g_2'$, lead to the most visible structures, referred to as "broaden emission lines" in [26]. In these graphs we do not show the transition $E_{1,21} \rightarrow E_{2',21'}$, which occurs at higher energy.

Interesting surface-states effects were unveiled and the eigenfunctions' parity and subband symmetries role, on the selection rules and leading order rules, were shown. High-accuracy PL experimental results, with features that could not be explained before,²⁷ are now fully understood. The improved optical response theory opens up the possibility to enhance the optical techniques for specific applications. We expect that the relation between surface states, cladding layers' energy gap and the novel group structure and isolated peak in the PL spectra, will be further studied and experimentally confirmed.

The author acknowledges useful comments of H. P. Simanjuntak, A. Robledo-Martinez, J. Grabinsky and E. Ley-Koo.

¹ More than 50 years ago, Leo Esaki noticed that while the real SLs contain a finite number of layers ..., the standard theoretical approaches tacitly assume that the SLs are infinite-periodic structures. See L. Esaki, in *Heterojunctions and Semiconductor Superlattices: Proceedings of the Winter School Les Houches* Ed. by Guy Allan and Gerald Bastard, France, March 12-21, 1985.

² G. Bastard, *Wave Mechanics Applied to Semiconductor Heterostructures*, (Les Editions de Physique, Les Ulis Cedex, France 1988)

³ R. Dingle, W. Wiegmann and C. H. Henry, *Phys. Rev. Lett.* **33**, 827-830 (1974).

⁴ D. Mukherji and B. R. Nag, *Phys. Rev. B* **12**, 4338-4345 (1975).

⁵ R. Dingle, *Festkörper Probleme XV, Advances in Solid State Physics*, (Ed. H. J. Queisser, Pergamon and Vieweg & Sohn, Stuttgart 1975).

⁶ G. A. SaiHalasz, L. L. Chang, J.-M. Welter, C.-A. Chang and L. Esaki *Sol. Stat. Comm.* **27**, 935-937 (1978).

⁷ Y. Ch. Chang and J. N. Schulman, *Appl. Phys. Lett.* **43**,

- 536-538 (1983).
- ⁸ H. Luo and J. K. Furdyna, *Phys. Rev. B* **41**, 5188-5196 (1990).
- ⁹ G. Yang, S. Lee and J. K. Furdyna, *Phys. Rev. B* **61**, 10978-10984 (2000).
- ¹⁰ M. Helm et al., *Phys. Rev. B* **48**, 1601-1606 (1993).
- ¹¹ H. Haug and S. W. Koch, Quantum theory of the optical and electronic properties of semiconductors (4th. Ed. World Scientific, Singapore 2004).
- ¹² Y. B. Band, *Light and matter: electromagnetism, optics, spectroscopic and lasers*, John Wiley & Sons Ltd. (2006), and references therein.
- ¹³ M. Virgilio, et al., *Phys. Rev. B* **79**, 075323 (2009).
- ¹⁴ M. Helm et al., *Phys. Rev. B* **43**, 13983-13991 (1991).
- ¹⁵ L. W. Molenkamp et al., *Phys. Rev. B* **38**, 6147 (1988).
- ¹⁶ G. D. Sanders and Y. Ch. Chang, *Phys. Rev. B* **32**, 5517 (1985).
- ¹⁷ W. T. Masselink et al., *Phys. Rev. B* **32**, 8027 (1985).
- ¹⁸ D. C. Reynolds et al., *Phys. Rev. B* **37**, 3117 (1988).
- ¹⁹ Y. Fu and K. A. Chao, *Phys. Rev. B* **40**, 8349 (1989).
- ²⁰ W. Zhu et al., *J. Phys: Condens. Matter* **7**, 9693 (1995).
- ²¹ S. Nakamura, S. Pearton and G. Fasol, *The Blue Laser Diode. The complete history* (Springer-Verlag, Berlin Heidelberg 1997), see pages 247, 261, 268, for example.
- ²² P. Pereyra, *Ann. Phys.* **320**, 1-20 (2005).
- ²³ P. Pereyra, arXiv condmatt 1607.02685.
- ²⁴ P. Pereyra, arxiv condmatt 1607.02686.
- ²⁵ S. Nakamura et al., *App. Phys. Lett.* **68**, 3269-3271 (1996).
- ²⁶ S. Nakamura et al. *Jpn. J. Appl. Phys.* **35**, L217 (1996)
- ²⁷ See for example pp 247 and 268 of Ref. [21].